Talanta 82 (2010) 1126–1135

Contents lists available at ScienceDirect

Talanta

journal homepage: www.elsevier.com/locate/talanta

Nickel oxide nanotubes-carbon microparticles/Nafion nanocomposite for the electrooxidation and sensitive detection of metformin

N. Sattarahmady [a], H. Heli [b,*], F. Faramarzi [c]

[a] Department of Biochemistry, Shiraz University of Medical Sciences, Shiraz, Iran
[b] Laboratory of Analytical and Physical Electrochemistry, Department of Chemistry, Islamic Azad University, Fars Science and Research Branch, 73715-181 Marvdasht, Iran
[c] Department of Chemistry, K. N. Toosi University of Technology, Tehran, Iran

ARTICLE INFO

Article history:
Received 5 April 2010
Received in revised form 11 June 2010
Accepted 17 June 2010
Available online 25 June 2010

Keywords:
Metformin
Nickel oxide
Nanotubes
Nanocomposite
Electrocatalysis

ABSTRACT

The electrocatalytic oxidation of metformin was studied on a nickel oxide nanotubes-carbon microparticles/Nafion nanocomposite, using cyclic voltammetry and chronoamperometry. In the presence of metformin, the anodic peak current of the Ni(II)/Ni(III) transition increased, followed by a decrease in the corresponding cathodic currents. Based on the results, the drug was oxidized on nickel oxide nanotubes via an electrocatalytic mechanism. The catalytic rate constant, the electron transfer coefficient and the diffusion coefficient involved in the electrocatalytic oxidation of the drug were reported. A sensitive and efficient amperometric method was presented for the analysis of the drug, and the corresponding analytical parameters were reported. For metformin, a detection limit of 0.45 μmol L^{-1} was obtained. The proposed amperometric method was also applied to the analysis of commercial tablets and the results were in good agreement with the declared values. Also, the applicability of the method to the direct assays of the drug in human serum and urine and breast milk was described.

1. Introduction

Diabetes and its abnormalities are a major health problem in the modern society. It is characterized by disruption of insulin production, leading to high blood glucose concentration and other complications such as neuropathy, renal dysfunction and cardiopathy [1]. The two categories of diabetes mellitus are type I (insulin-dependent) and type II (non-insulin dependent). Type II diabetes is a progressive and complex disease that is difficult to manage effectively in the long-term. Metformin, N,N-dimethylimidodicarbonimidic diamide (Scheme 1) is an orally administered antihyperglycemic drug used to treat type II diabetes. It helps diabetics to control the amount of glucose (sugar) to a normal level and maintains this level in their blood. Metformin can be used alone or in conjunction with other medications, sulfonylureas, alpha-glucosidade inhibitors, or insulin. Although metformin's exact mechanism of action is not completely understood, it decreases the intestinal absorption of dietary carbohydrates, inhibits hepatic glucose production and gluconeogenesis or, perhaps most importantly, increases the sensitivity of muscle cells to insulin by enhancing peripheral glucose uptake and utilization [2].

A variety of separation techniques have been proposed for assay determination of metformin. These include gas chromatography with electron-capture [3] or mass spectrometry detection [4], capillary electrophoresis [5], conductometry [6] and voltammetry [7–9]. Several methods of analysis by high performance liquid chromatography (HPLC) have also been published for the determination of metformin using various separation modes, such as reverse-phase [10], ion-pair [11], cation exchange [12] and normal-phase [13]. However, some of these methods suffer from several disadvantages, namely sensitivity, long chromatographic run times or a cumbersome extraction procedure before analysis which prevent their use for routine sample analysis. For example, HPLC methods have exhibited low sensitivity [13,14] and require relatively large sample volumes [15,16], complicated sample preparation procedures including evaporation steps [16,17], long chromatographic times [18], long analytical columns and conventional mobile phase flow rates [13–18].

Electrochemical techniques have been shown to be excellent procedures for the sensitive determination of drugs and related compounds in pharmaceutical dosage forms and biological fluids [19–22]. The advance in electrochemical techniques in the field of drug analysis is due to their simplicity, high sensitivity, low cost, and relatively short analysis time compared to the other techniques. The specificity and selectivity of the voltammetric techniques are usually excellent because the analyte can be readily identified by its voltammetric peak potential. Moreover,

* Corresponding author. Tel.: +98 728 46 92 114; fax: +98 728 46 92 153.
E-mail address: hheli7@yahoo.com (H. Heli).

0039-9140/$ – see front matter © 2010 Elsevier B.V. All rights reserved.
doi:10.1016/j.talanta.2010.06.022

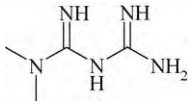

Scheme 1. Chemical structure of metformin.

electrochemistry is most suitable for investigating the redox properties of drugs that can give insight into its metabolic fate. The data obtained from electrochemical techniques are often correlated with molecular structures and pharmacological activities of drugs.

Electrochemistry of metformin has been slightly investigated. Tian et al. [7] studied the electrochemistry of metformin on a carbon paste electrode modified with a copper(II) coordination polymer-carbon nanotube. Skrzypek et al. [8] employed mercury electrode for electroreduction and determination of metformin. Also, Tian and Song [9] determined metformin in pharmaceuticals using the promotion effect of copper(II) ion on its oxidation current on the surface of a carbon paste electrode. However, these studies were involved in determination of metformin at highly positive or negative potentials which common interferences can interfere with the analysis procedure. In addition, mercury as the working electrode is toxic and is not suitable for the analysis in flowing systems. Solid electrodes which were employed represented slow kinetics and can also be fouled up with the reaction intermediates/products of the electrooxidation reactions. This causes low sensitivity and reproducibility. Thus, there is still a need to develop other electrode materials that can detect metformin in pure and pharmaceutical forms as well as analysis in biological fluids.

Nanomaterials possess unique properties in various fields on account of different effects in terms of volume, quantum size, surface and macroscopic quantum tunnel [23]. These unique properties and improved performances which are determined by their size, structure, and mutual interaction among the nanostructured species lead to their applicability in sensing and biosensing areas. Metal oxide nanoparticles have received tremendous attention due to their unique properties such as conductivity, magnetism, catalysis and electrocatalysis in comparison with their bulk counterparts [24–27]. Among them, nanosized nickel oxide has received a considerable amount of attention as a promising material due to large surface area, high conductivity, efficient catalytic activity and excellent electrochemical properties [28,29]. In this regard, considerable efforts have been focused on the synthesis of nickel and nickel oxide nanostructures [28–31]. However, new strategies for designing nickel oxide nanostructures and nanocomposites to further improve their electrochemical activity are still interesting to be used.

Carbon composite electrodes (CCEs) have been widely employed in electrochemical studies due to the vast advantages of low cost, ease of fabrication, miniaturization, surface renewability, tunability, and wide potential window [25–28,32,33]. In addition, CCEs can be fabricated using various compounds such as metals, metal oxides and biomacromolecules to perform mechanistic studies and the selectivity and sensitivity in electroanalysis studies [25–28,32–34]. The incorporation of metal and metal oxide particles in the carbon composites offers a homogeneous and stable medium of the immobilization of catalytic metal and metal oxide centers. The metal and metal oxide-based CCEs bear advantages of both carbon properties and electrocatalytic reactivity of metal and oxide surfaces.

In the present study, we investigated the electrocatalytic oxidation and sensitive determination of metformin at a nickel oxide nanotubes-carbon microparticles/Nafion nanocomposite. To the best of our knowledge, this procedure has not been carried out successfully so far.

2. Experimental

2.1. Reagents

All chemicals used in this work were of analytical grade from Merck (otherwise those stated) and were used without further purification. Nafion solution was purchased from Sigma. Multiwall carbon nanotubes (MWCNTs) were obtained from PlasmaChem GmbH, Germany. Carbon microparticles (graphite fine powder) with a particle size of less than 50 μm were obtained from Merck. All the solutions were prepared by redistilled water. Metformin was obtained from the Center of Quality Control of Drug, Tehran, Iran. The metformin tablets/capsules/oral solution was obtained from a local drugstore.

2.2. Apparatus

Electrochemical measurements were carried out in a conventional three-electrode cell powered by an μ-Autolab (The Netherlands). The system was run on a PC using GPES 4.9 software. A saturated Ag/AgCl and a platinum disk were used as the reference and counter electrodes, respectively.

To obtain information about the morphology and size of the particles, scanning electron microscopy (SEM) was performed using a X-30 Philips instrument and transmission electron microscopy (TEM) was performed using a CEM 902A ZEISS instrument with an accelerating voltage of 80 kV. For TEM, the samples were prepared by placing a drop of the particles, dispersed in ethanol, on a carbon-covered nickel grid (400 mesh) and evaporating the solvent.

Atomic absorption was measured using a GBC 932 instrument equipped with a graphite furnace.

2.3. Preparation of nickel oxide nanotubes

Nickel oxide nanotubes were synthesized using the scaffold of MWCNTs. MWCNTs were firstly pretreated as described previously [35]. Briefly, MWCNTs were refluxed in a 2.0 mol L^{-1} nitric acid solution for 12 h, washed with redistilled water several times, then dried and stored until use. Then, MWCNTs were sonicated in a 3:1 sulfuric/nitric acid solution for 6 h in an ultrasonic bath at room temperature and then washed with distilled water until neutralization by vacuum filtration. The obtained sample was taken, and dried overnight at 50 °C. This procedure causes scission and carboxylation of MWCNTs and therefore, they acquire negative charges on the outside of the tubes. An aqueous solution of nickel nitrate was prepared separately and mixed with 200 mg of pretreated MWCNT. The mixture was sonicated and then heated in an oven at 80 °C for 15 min and continued to heat to dry the sample. Then, the dried mixture was put into a microwave worked at 2.45 GHz and a fixed power level of 850 W. The mixture was 20 s irradiated following by a 60 s rest and the microwave irradiation procedure was repeated ten times to produce nickel oxide nanotubes. Based on the atomic absorption measurements, 5.8 ± 0.3 mg of nickel was deposited on 1 mg of MWCNT.

2.4. Preparation of nickel oxide microparticles

In order to do a comparison, nickel oxide microparticles were synthesized using the scaffold of carbon microparticles in a similar fashion; otherwise, carbon microparticles were employed instead of MWCNTs.

2.5. Preparation of the working electrodes

Carbon paste electrode (CPE) was prepared by hand-mixing carbon microparticles and mineral oil with an 80/20% (w/w) ratio. The

paste was carefully mixed and homogenized in an agate mortar for 20 min. The resulting paste was kept at room temperature in a desiccator before use. The paste was packed firmly into a cavity (4.05 mm diameter, geometric surface are of 0.128 cm^2 and 0.5 mm depth) at the end of a Teflon tube. Electrical contact was established via a copper wire connected to the paste in the inner hole of the tube. The electrode surface was gently smoothed by rubbing on a piece of weighing paper just prior to use. This procedure was also used to regenerate the surface of CPE.

Nickel oxide microparticles-carbon microparticles composite was prepared by hand-mixing carbon microparticles, mineral oil and nickel oxide microparticles with a 64/20/16% (w/w) ratio. Nickel oxide microparticles-carbon microparticles/Nafion composite (m-NC) was prepared by covering nickel oxide microparticles-carbon microparticles composite with 10 μL of a 2% (w/v) low aliphatic alcohols Nafion solution. m-NC was then transferred to a 100 mmol L^{-1} NaOH solution and 25 consecutive cyclic potentials were done in a regime of cyclic voltammetry in a range of 350–750 mV at a potential sweep rate of 100 mV s^{-1}. This procedure leads to some structural changes and transformation of the nickel oxides to stable forms.

Nickel oxide nanotubes-carbon microparticles nanocomposite was prepared by hand-mixing carbon microparticles, mineral oil and nickel oxide nanotubes with a 64/20/16% (w/w) ratio. Nickel oxide nanotubes-carbon microparticles/Nafion nanocomposite (n-NC) was prepared by covering nickel oxide nanotubes-carbon microparticles nanocomposite with 10 μL of a 2% (w/v) low aliphatic alcohols Nafion solution. Similar polarization pretreatment was also applied to n-NC.

2.6. Procedures

Standard solutions of the drug were prepared by dissolving an accurate mass of the bulk drug in an appropriate volume of 100 mmol L^{-1} NaOH solution (which was also used as the supporting electrolyte). All the solutions were kept in the dark at 4 °C and were used within 24 h to avoid decomposition. Additional dilute solutions were prepared daily by accurate dilution just before use.

The calibration curve for the drug in 100 mmol L^{-1} NaOH solution was measured with an amperometric technique. The working potential of 660 mV was used in amperometric measurements, in which the transient currents were allowed to decay to steady-state values.

All the studies/measurements were carried out at room temperature.

2.7. Metformin tablet assay procedure

For analysis of the tablets, the average weight of ten tablets from each sample was determined; then, the tablets were finely powdered and homogenized in a mortar. Appropriate and accurately weighed amounts of the homogenized powder were transferred into 100 mL calibrated flasks containing 50 mL of 100 mmol L^{-1} NaOH solution. The contents of the flasks were sonicated for 30 min, and then the undissolved excipients were removed by filtration and diluted to volume with the same supporting electrolyte. Appropriate solutions were prepared by taking suitable aliquots of the clear filtrate and diluting them with 100 mmol L^{-1} NaOH solution.

2.8. Analysis of spiked urine, blood serum and breast milk samples

The drug-free serum samples were obtained from healthy male volunteers and stored frozen until the assay. The serum samples were diluted (1:7) with the supporting electrolyte and filtrated through a 30 kDa filter to produce protein-free human serum. Various portions of the stock drug solutions were transferred into 10 mL volumetric flasks containing 3.3 mL of the serum sample. These solutions were then diluted to the mark with the supporting electrolyte for preparation of spiked samples (final dilution of 1:20 with the supporting electrolyte). The spiked serum solutions were directly analyzed by the calibration method, according to our proposed amperometry method.

The urine samples taken from a healthy person were diluted (1:10) with the supporting electrolyte after adding an appropriate amount of the drug standard solution. The resulting solutions were then directly analyzed, according to our proposed procedure without any pretreatment or extraction steps.

The breast milk samples were diluted (1:10) with the supporting electrolyte after adding an appropriate amount of the drug standard solution. Then, the resulting solutions were then directly analyzed.

2.9. Recovery experiments

Because other components of the matrix of the pharmaceutical dosage forms and biological fluids may interfere with the analysis or accurate quantitation of the analyte, potential effects from matrix components must be investigated. In this regard, recovery experiments are performed in the presence of the real matrices using the standard addition method. In order to know whether the matrices show any interference with the analysis, known amounts of metformin were added to the pre-analyzed dosage forms and biological fluids. The mixtures were analyzed by the amperometry method.

3. Results and discussion

3.1. Electron microscopy

Fig. 1A shows SEM image of the nickel oxide nanotubes. Nickel oxide nanotubes were formed as bundles and twisted together. Fig. 1B and C show TEM images of MWCNT and the nickel oxide nanotubes, respectively. It can be seen that the long filum of MWCNTs are relatively twisted together and have an average diameter of 20–40 nm and of 0.5–1 μm length. Nickel oxide precipitated on the outside of the tubes of MWCNTs and covered the "hard template" of MWCNTs as a shell and formed nanotubes of nickel oxide. The average thickness of the nanotubes of nickel oxide was about 25 nm.

3.2. Study of the charge transfer kinetics across the n-NC/solution interface

Fig. 2A shows cyclic voltammograms of n-NC in 100 mmol L^{-1} NaOH solution recorded at a wide range of potential sweep rates, from 3 to 750 mV s^{-1}. A pair of well-defined peaks with a mid-peak potential of 575 mV appeared in the voltammograms, and the peak-to-peak potential separation (at the potential sweep rate of 10 mV s^{-1}, Fig. 2A, inset) was 170 mV. The voltammograms shown are similar to those previously reported [36–38], and the redox transition involved is attributed to the presence of Ni(II)/Ni(III) species immobilized at the electrode surface via the following reaction [28,36,37]:

$$NiOOH + H_2O + e \rightleftarrows Ni(OH)_2 + OH^- \quad (1)$$

The peak-to-peak potential separation in the voltammograms deviated from the theoretical value of zero and increased at higher potential sweep rates. This result indicates a limitation in the charge-transfer kinetics, which is due to: (a) chemical interactions between the electrolyte ions and the nickel species, (b) dominance of electrostatic factors, (c) the lateral interactions of the redox couples present on the surface and/or (d) non-equivalent sites present in the nickel species.

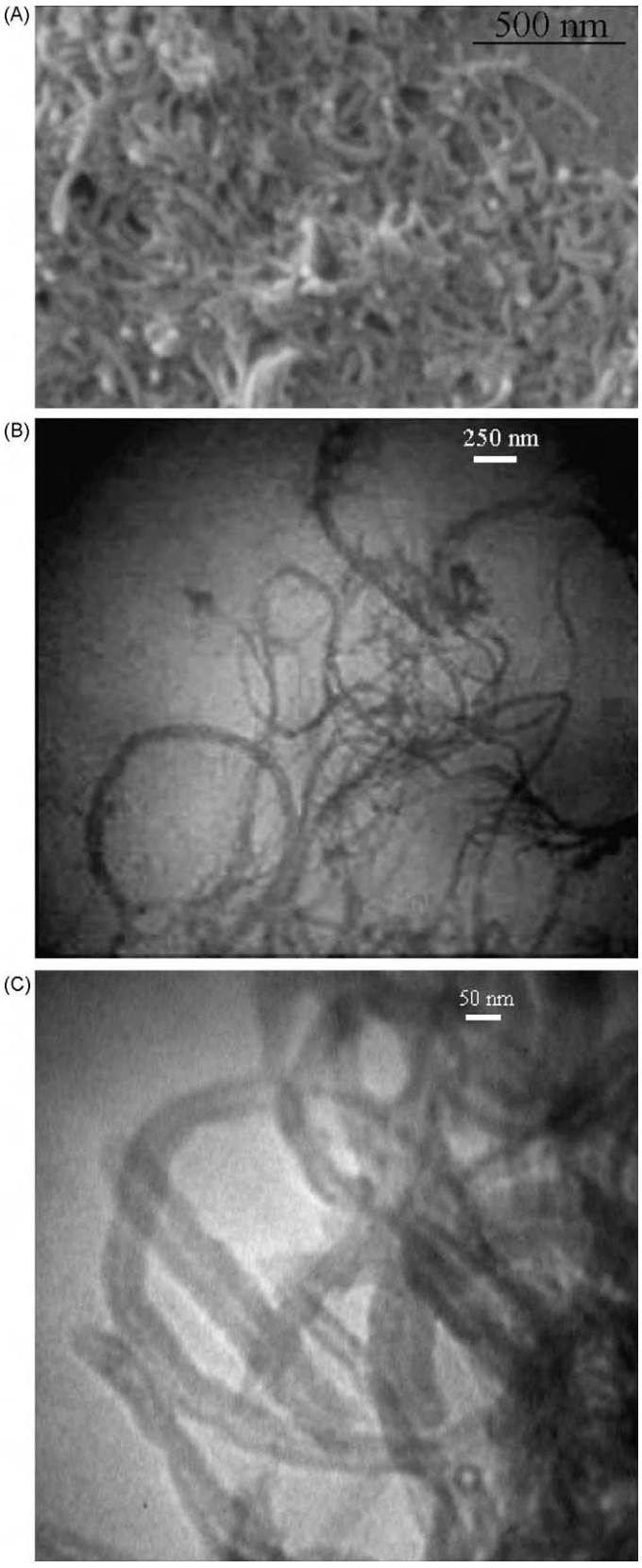

Fig. 1. A SEM image of the nickel oxide nanotubes (A), TEM images of MWCNT (B) and the nickel oxide nanotubes (C).

Laviron derived general expressions for the linear potential sweep voltammetric response of surface-confined electro-reactive species at small concentrations [38]. The expressions for the peak-to-peak potential separation (ΔE_p) > 200/n mV, where n is the number of exchanged electrons, are as follows:

$$E_{pa} = E^{0'} + X \ln\left[\frac{(1-\alpha_s)}{m}\right] \quad (2)$$

$$E_{pc} = E^{0'} + Y \ln\left[\frac{\alpha_s}{m}\right] \quad (3)$$

$$\ln k_s = \alpha_s \ln(1-\alpha_s) + (1-\alpha_s)\ln\alpha_s - \ln\left(\frac{RT}{nF\nu}\right) - \alpha_s(1-\alpha_s)\frac{nF\Delta E_p}{RT} \quad (4)$$

where $X = RT/(1-\alpha_s)\,nF$, $Y = RT/\alpha_s nF$, $m = (RT/F)(k_s/n\nu)$, E_{pa} and E_{pc} are the anodic and cathodic peak potentials, respectively, and α_s, k_s and ν are the electron-transfer coefficient, apparent charge-transfer rate constant and potential sweep rate, respectively. From these expressions, α_s can be determined by measuring the variation of the peak potential with respect to the potential sweep rate, and k_s can be determined for electron transfer between the electrode and the surface-deposited layer by measuring the ΔE_p values. Fig. 2B shows the plot of $(E_p - E^{0'})$ with respect to the logarithm ν from the cyclic voltammograms represented in Fig. 2A for the anodic and cathodic peaks. It can be observed that for the potential sweep rates of 300–750 mV s^{-1}, the values of $(E_p - E^{0'})$ linearly depend on the logarithm of the potential sweep rate indicated by Laviron. Using the plot and Eqs. (2)–(4), the value of α_s was obtained as 0.52 ± 0.03. Moreover, the mean value of k_s was obtained as 4.62 ± 0.07 s^{-1}. This is higher than those reported elsewhere in the literature [37,39] for the redox process of nickel species generated from nickel bulk metal. This result indicates that the nickel oxide nanotubes represent a higher electron-transfer rate in the redox process of nickel species in alkaline solution compared to the microstructures represented in Refs. [37,39]. The voltammograms represented in Fig. 2A also show that the anodic and cathodic peak currents depend linearly on the potential sweep rate at low values of 3–20 mV s^{-1} (Fig. 3A and C). This result is attributable to the electrochemical activity of an immobilized redox couple at the surface. From the slope of these lines and using [40],

$$I_p = \left(\frac{n^2F^2}{4RT}\right)\nu A\Gamma* \quad (5)$$

where I_p is the peak current, A is the electrode surface area and Γ^* is the surface coverage of the redox species. Taking the average of both cathodic and anodic currents, a total surface coverage of the electrode by the nickel species of about $4.99 \pm 0.06 \times 10^{-8}$ mol cm^{-2} was derived. In the higher range of potential sweep rates of 30–750 mV s^{-1} (Fig. 3B and D), this dependency is of square-root form, signifying the dominance of a diffusion process as the rate-limiting step in the total redox transition of the nanocomposite. This limiting-diffusion process, which has been also reported for some other Ni-based modified electrodes [28,36,37], may be due to the charge neutralization during the oxidation/reduction process.

3.3. Electrocatalytic oxidation of metformin

Fig. 4 shows cyclic voltammograms of CPE (A), m-NC (B) and n-NC (C) in the supporting electrolyte in the absence (curve a) and presence (curve b) of 20 μmol L^{-1} metformin at a potential sweep rate of 10 mV s^{-1}. Metformin is electroinactive on carbon electrodes and represent no anodic signal using CPE in the swept potential range in 100 mmol L^{-1} NaOH solution. m-NC and n-NC represented similar signatures in the voltammograms related to Ni(II)/Ni(III) redox transition. Metformin was oxidized on both m-NC and m-NC and the voltammograms represent enhancement in the anodic currents (and the corresponding charges) and decrements in the

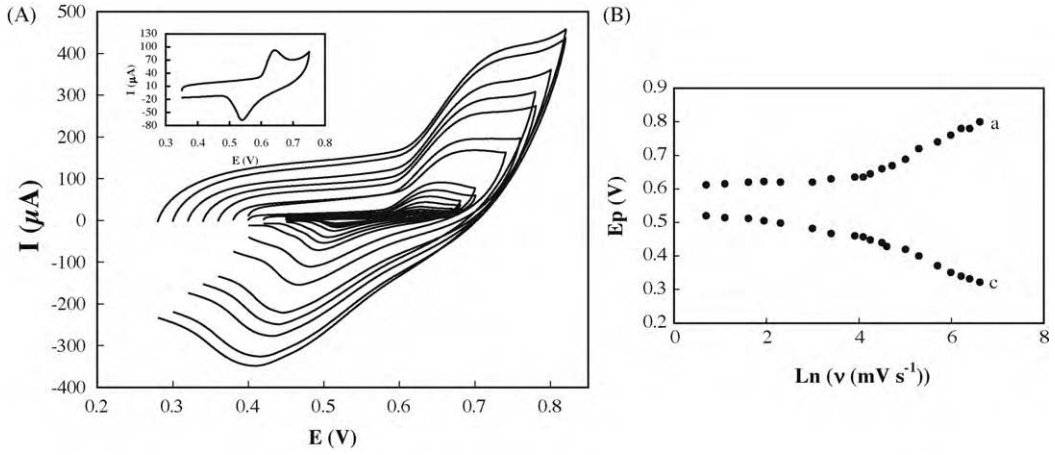

Fig. 2. (A) Cyclic voltammograms of n-NC in 100 mmol L^{-1} NaOH solution recorded at a wide range of potential sweep rates, from inner to the outer of 3, 5, 7, 10, 20, 30, 50, 60, 70, 90, 100, 150, 200, 300, 400, 500, 600 and 750 mV s^{-1}. Inset: Typical cyclic voltammogram of n-NC in 100 mmol L^{-1} NaOH solution recorded at 10 mV s^{-1}. (B) Plot of $(E_p - E^{0\prime})$ with respect to the logarithm ν for the anodic (a) and cathodic (c) peaks.

cathodic currents (and the corresponding charges). From the cyclic voltammograms represented in Fig. 4, an electrocatalytic mechanism for the electrooxidation of metformin on the composites can be deduced in which the redox transition of the nickel species,

$$Ni(II) \rightleftarrows Ni(III) + e \quad (6)$$

was followed by the oxidation of metformin via the following reaction:

$$Ni(III) + Metformin \xrightarrow{k_{cat}} Product(s) + Ni(II) \quad (7)$$

Regarding the product(s) of the electrocatalytic oxidation of metformin on n-NC, it should be noted that metformin bears two types of functional groups of amine (primary, secondary and tertiary) and imine. For the electrooxidation of amines on copper- and nickel-based electrodes, the following mechanism has been reported [41–43]:

(for primary straight chain amines)

$$RCH_2NH_2 \rightarrow RCH = NH + 2e + 2H^+ \quad (8)$$

$$RCH = NH \rightarrow RC \equiv N + 2e + 2H^+ \quad (9)$$

$$\{RCH = NH + H_2O \rightarrow RCH = O + NH_3\} \quad (10)$$

(for primary branched chain amines)

$$R_1CH(R_2)NH_2 \rightarrow R_1C(R_2) = NH + 2e + 2H^+ \quad (11)$$

$$\{R_1C(R_2) = NH + H_2O \rightarrow R_1C(R_2) = O + NH_3\} \quad (12)$$

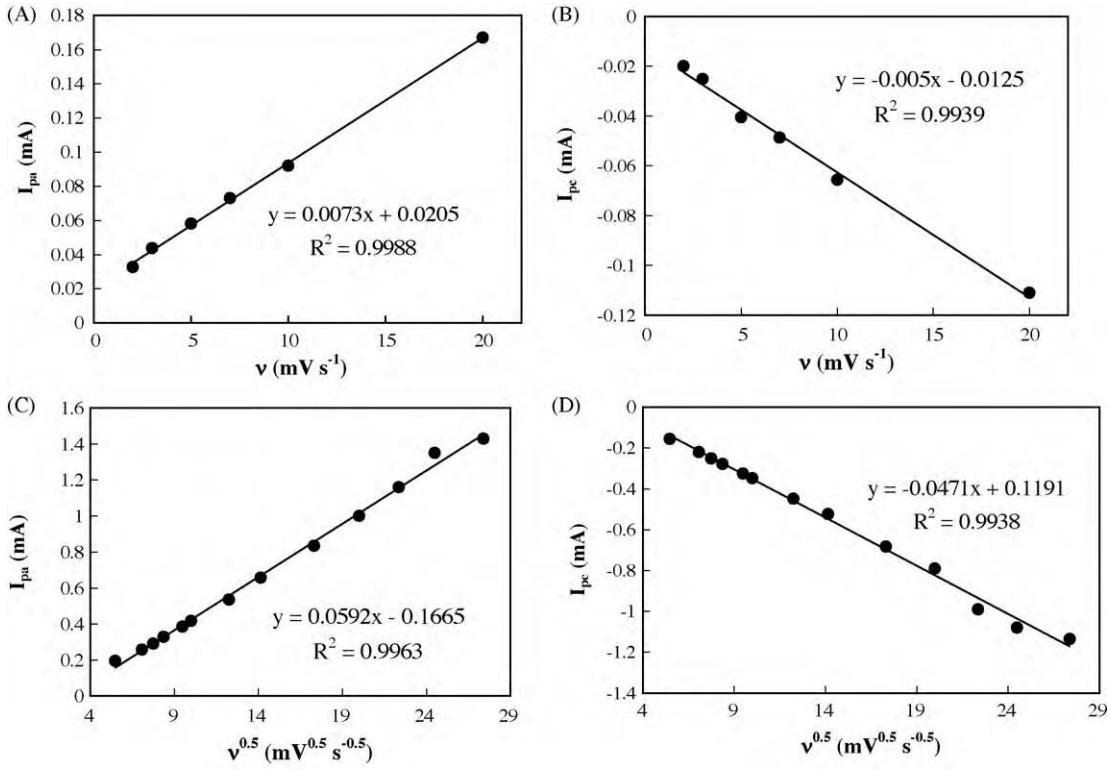

Fig. 3. Dependency of anodic (A) and cathodic (C) peak currents of the cyclic voltammograms shown in Fig. 2A on the potential sweep rate at low values of 3–20 mV s^{-1} and dependency of anodic (B) and cathodic (D) peak currents on the square root of the potential sweep rate at high values of 30–750 mV s^{-1}.

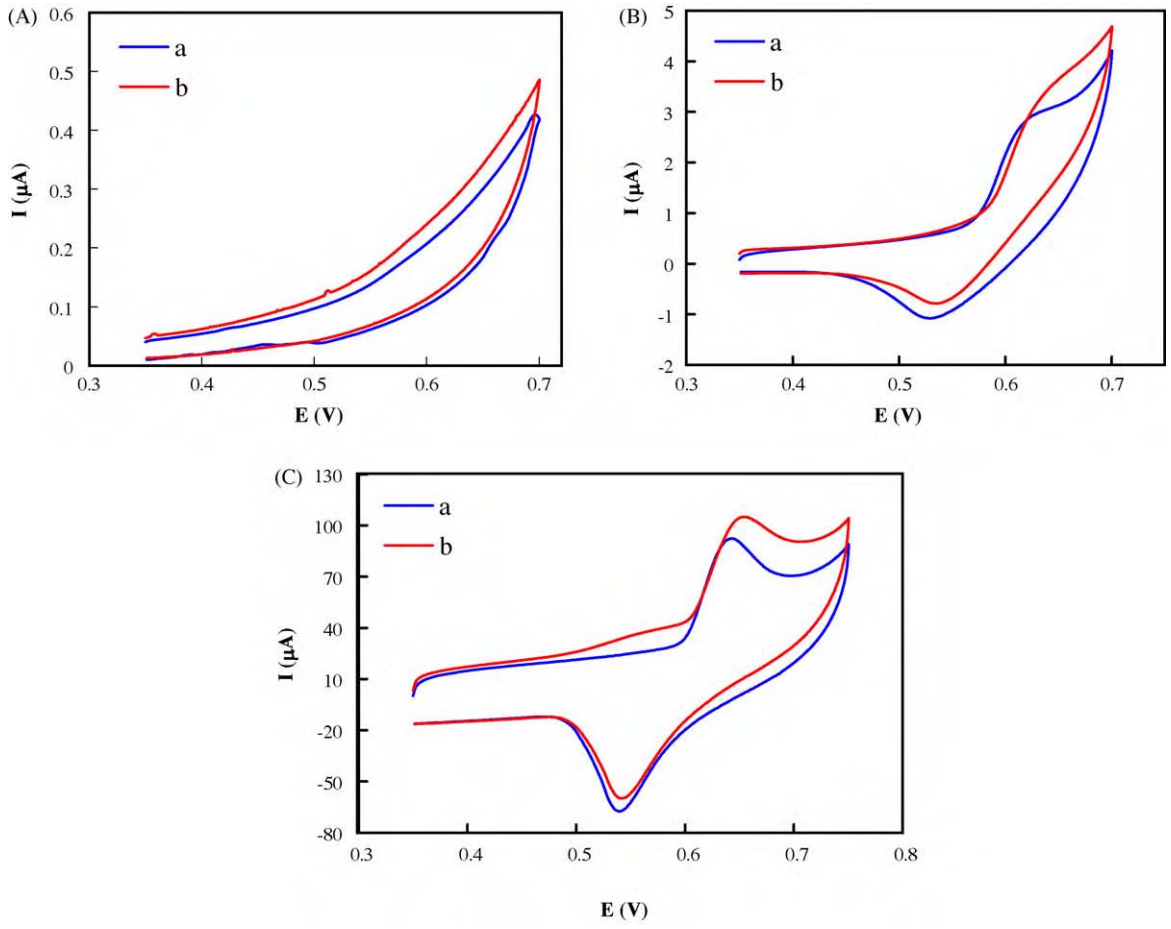

Fig. 4. Cyclic voltammograms of CPE (A), m-NC (B) and n-NC (C) in the supporting electrolyte in the absence (curve a) and presence (curve b) of 20 μmol L^{-1} metformin at a potential sweep rate of 10 mV s^{-1}.

and (for secondary amines)

$$(RCH_2)_2NH + H_2O \rightarrow RCH=O + RCH_2NH_2 + 2e + 2H^+ \quad (13)$$

According to these mechanisms, primary linear chain amines (in which the amine group is connected to a first type carbon) are oxidized in two two-electron steps and produce the corresponding imine and nitril, respectively. Also, the primary branched-chain amines (in which the amine group is connected to a second type carbon) are oxidized in a single two-electron step and the corresponding imine is the unique product. It should be also added that the nitrils can hydrolized slowly to cetons.

For the electrooxidation of imines, the following mechanism based on the similarities between enzymatic and electrodic processes can be proposed [44]:

$$RCH=NHH_2O \rightarrow RCH=NOH + 2e + 2H^+ \quad (14)$$

$$\{RCH=NOH + H_2O \rightarrow RCH=O + NO + 3e + 3H^+\} \quad (15)$$

Another point in curve b in Fig. 4C is that in the voltammogram, an anodic peak located at 570 mV (prior to the anodic current related to the electrocatalytic oxidation of this drug via a higher-valence nickel moiety) is also observed. This peak is absent using CPE in the presence of the drug and also using n-NC in the absence of the drug. Therefore, the peak is involved in the electrooxidation of metformin on n-NC. This peak may be a pre-peak for the major electrocatalytic peak which can be related to the adsorption of the reaction product(s) on the electrode surface. The reaction product(s) can be different compounds (vide supra) and some compounds may simultaneously be adsorbed on the electrode surface. However, it does not cause any surface fouling effect (vide infra).

In an electrocatalytic reaction based on surface-confined mediated electron transfer, the electrocatalytic efficiency is dependent on both kinetics of charge transfer process of the redox mediator itself, as well as catalytic rate constant of the chemical reaction occurring between the mediator and the substrate [26,37]. On the other hand, it is well-known that the overall reactivity of an electrocatalyst can have size- and shape-dependencies [20,27,28,32,33,45,46]. In this regard, although nickel-based composites show similar signatures in the cyclic voltammograms and the voltammograms represented here are similar to those reported for other nickel-based electrodes [28,29,36,37], the currents in the voltammograms using n-NC are much higher. Although both composites are fabricated using the same mass of active nickel species, the nanotubes of nickel oxide can represent a higher surface area and/or the nanosize effect. From the cyclic voltammograms represented in Fig. 4B and C, it can be seen that the currents were higher for n-NC compared to m-NC. This can be initially related to the higher surface area of n-NC. Therefore, it will cause higher sensitivity for the amperometric sensor constructed based on n-NC (vide infra). On the other hand, the surface effect-free catalytic efficiencies for the composites (for the same concentration of metformin) can be calculated as: $(I_{metformin} - I_b)/I_b$, where $I_{metformin}$ is the anodic current in the presence of metformin and I_b is the base anodic current. These catalytic efficiencies were obtained as 0.17 ± 0.04 and 0.24 ± 0.04 for m-NC and n-NC, respectively. This will also cause a higher sensing utility which is due to the nature of the nickel oxide nanotubes. However, the higher catalytic effi-

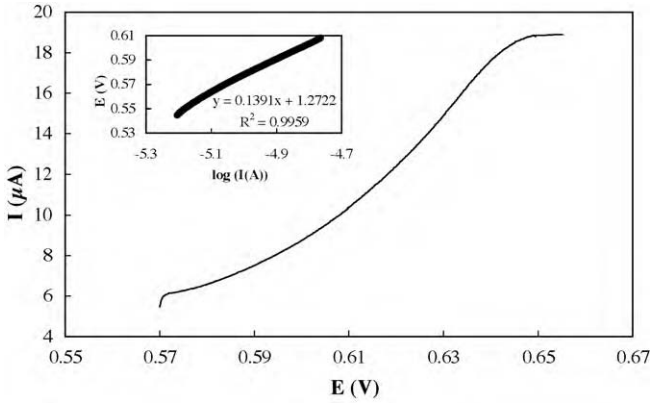

Fig. 5. A steady-state current–potential curve recorded for the electrocatalytic oxidation of metformin on n-NC. Inset: The corresponding Tafel plot.

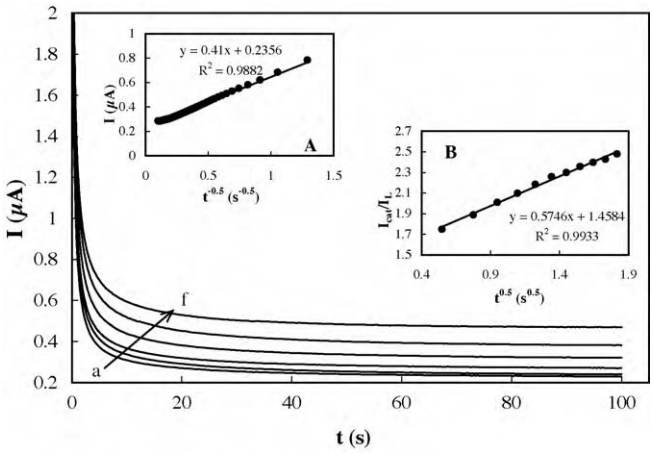

Fig. 6. Chronoamperograms recorded in different concentrations of: (a) 0, (b) 0.03, (c) 0.05, (d) 0.1, (e) 0.3 and (f) 0.5 mmol L^{-1} metformin using n-NC. The potential step was 660 mV. Inset A: Dependency of transient current on $t^{-0.5}$ related to curve e in main panel. Inset B: Dependence of I_{cat}/I_L on $t^{0.5}$ related to curve e in main panel.

ciency of n-NC is related to the nanosize effect of n-NC and the higher apparent charge-transfer rate constant.

Cyclic voltammograms of n-NC in a wide range of potential sweep rates of 3–750 mV s^{-1} in the presence of 0.5 mmol L^{-1} metformin were recorded. Upon increasing the potential sweep rate, the anodic peak current increased and depended linearly on the square root of the potential sweep rate (supplementary material S1). This linear dependency indicates the domination of a diffusion-controlling step for the electrooxidation process. Another point is that plotting the current function (peak current divided by the square root of the potential sweep rate) against the square root of the potential sweep rate revealed a negative slope (supplementary material S1). This further confirms the electrocatalytic nature of the process.

The effect of the presence of Nafion in the composite was also investigated by cyclic voltammetry. Nafion does not influence the current because it is negatively charged, while metformin is neutral in the working pH. However, Nafion can have an important role on the selectivity of the electrochemical sensors and biosensors [26,28]. Cyclic voltammograms of nickel oxide nanotubes-carbon microparticles nanocomposite and n-NC in the presence of 0.5 mmol L^{-1} metformin were recorded (supplementary material S2). The voltammograms in the absence and presence of covered Nafion layer were nearly the same. Therefore, Nafion did not affect the electrooxidation process of metformin.

Fig. 5 shows a steady-state current-potential curve recorded for the electrocatalytic oxidation of metformin on n-NC. Typical S-shaped plot was obtained and the transfer coefficient (α) was obtained by plotting the potential versus logarithm of the pseudo-steady state current (Fig. 5, inset). The charge-transfer coefficient for the electrooxidation of metformin on the n-NC surface was obtained as $\alpha = 0.41 \pm 0.02$. This indicates a near-symmetric barrier for potential energy change during the electrooxidation process with a slightly curvature to the reaction products.

In order to further inspect the reaction mechanism and its kinetic, the oxidation of metformin on n-NC was investigated by chronoamperometry. Fig. 6 shows chronoamperograms recorded in the absence (curve a) and presence (curves b–f) of metformin using the potential step of 660 mV. The transient currents decayed with time in a Cotrellian manner. This indicates that the electrocatalytic oxidation of metformin on n-NC was controlled by diffusion in the bulk of solution. This was also confirmed by cyclic voltammetry (vide supra). By using the slope of the line represented in Fig. 6, inset A, the diffusion coefficient of metformin can be obtained according to Cottrell equation [40]:

$$I = nFAD^{1/2}C\pi^{-1/2}t^{-1/2} \quad (16)$$

where D is the diffusion coefficient, A is the electrode surface area and C is the bulk concentration. The mean value of the diffusion coefficient for metformin was found to be $5.61 \pm 0.04 \times 10^{-6}$ cm^2 s^{-1}.

Chronoamperometry can also be used for the evaluation of the catalytic rate constant according to the following equation [40]:

$$\frac{I_{cat}}{I_L} = \gamma^{1/2}\left[\pi^{1/2}erf(\gamma^{1/2}) + \frac{\exp(-\gamma)}{\gamma^{1/2}}\right] \quad (17)$$

where I_{cat} and I_d are the currents in the presence and absence of metformin, respectively, and $\gamma = k_{cat}Ct$ is the argument of the error function. k_{cat} is the catalytic rate constant and t is the elapsed time. In the cases where $\gamma > 1.5$, $erf(\gamma^{1/2})$ is almost equal to unity, the above equation can be reduced to:

$$\frac{I_{cat}}{I_L} = \gamma^{1/2}\pi^{1/2} = \pi^{1/2}(k_{cat}Ct)^{1/2} \quad (18)$$

From the slope of the I_{cat}/I_d vs. $t^{1/2}$ plot, presented in Fig. 6, inset B, the mean value of k_{cat} for the electrooxidation of metformin was obtained as $3.50 \pm 0.08 \times 10^4$ cm^3 mol^{-1} s^{-1}.

3.4. Determination of metformin

In order to develop a simple and time-saving procedure for the analysis of metformin in pure form, pharmaceutical formulation and spiked biological fluids, amperometry technique was employed. Typical amperometric signals obtained during successive increments of metformin to a 100 mmol L^{-1} NaOH solution using n-NC are depicted in Fig. 7. Gentle stirring for a few seconds was needed to promote solution homogenization after each injection. The electrode response is quite rapid and proportional to the metformin concentration. The corresponding calibration curve for the amperometric signals is shown in the inset of Fig. 7. The limits of detection (LOD) and quantitation (LOQ) of the procedure were calculated according to the 3 SD/m and 10 SD/m criteria, respectively, where SD is the standard deviation of the intercept and m is the slope of the calibration curves [47]. The determined parameters for calibration curves of the drug, accuracy and precision, LOD and LOQ and the slope of calibration curves are reported in Table 1. A comparison between the determined parameters for calibration curves of the drug was made in Table 2.

The applicability of the proposed amperometric method for the sample dosage form was examined by analyzing the tablets. It was found that the amounts of drug determined through this method

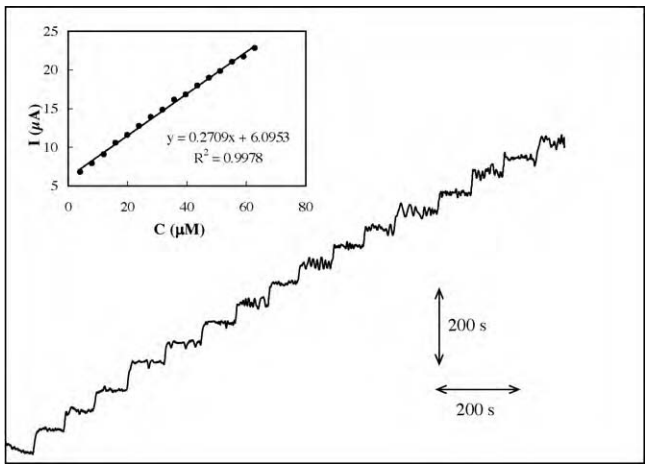

Fig. 7. Typical amperometric signals obtained during successive increments of metformin to a 100 mmol L^{-1} NaOH solution using n-NC. Inset: The corresponding calibration curve.

Table 1
The determined parameters for the calibration curves of metformin and accuracy and precision ($n = 3$) using n-NC.

Linear range (μmol L^{-1})	4.0–63
Slope (A (mol L^{-1})$^{-1}$)	0.27 ± 0.2
Intercept × 10^6 (A)	6.1 ± 0.8
R^2	0.998
LOD (μmol L^{-1})	0.45
LOQ (μmol L^{-1})	1.5
RSD (%)	2.7
Bias (%)	2.3

are in good agreement with the reported values. The values of experimentally determined drugs and declared values in tablets are tabulated in Table 3.

In order to evaluate the accuracy of this method and to know whether the excipients in pharmaceutical dosage form show any interference with the analysis, the proposed amperometric method was checked by recovery experiments using the standard addition method. After addition of the known amounts of pure drugs to various pre-analyzed formulations of the drugs, the mixtures were analyzed by the proposed method. The recoveries of the drugs were calculated using the corresponding regression equations of previously plotted calibration plots. The results of recovery experiments using the developed assay procedure are also presented in Table 3. The results indicate the absence of interference from commonly encountered pharmaceutical excipients used in the selected formulations. Therefore, the method can be applied for determination of the drugs in pharmaceutical forms without any interference from inactive ingredients.

Table 4
The determined parameters for the calibration curve of metformin spiked to human serum and urine and breast milk samples.

	Serum	Urine	Beast milk
Linear range (μmol L^{-1})	4.0–63	4.0–63	4.0–63
Slope (A (mol L^{-1})$^{-1}$)	0.13 ± 0.3	0.17 ± 0.12	0.18 ± 0.15
Intercept × 10^6 (A)	2.1 ± 0.07	0.28 ± 0.04	11.9 ± 4.2
R^2	0.99	0.99	0.99
LOD (μmol L^{-1})	0.95	0.61	0.69
LOQ (μmol L^{-1})	3.17	2.03	2.3
RSD (%)	3.9	3.6	2.2

The applicability of the proposed amperometric method for the determination of metformin in biological fluids of human serum blood, urine and breast milk was attempted. Amperometric signals were recorded for metformin spiked to serum, urine and breast milk samples using an applied potential of 660 mV. The results are listed in Table 4.

The percentage recovery of metformin was determined by comparing the currents of a known drug concentration in human serum, urine and breast milk with their equivalents in calibration curves; these results are also summarized in Table 5. Good recoveries of metformin were achieved from these matrices, denoting that application of our proposed amperometric method to the analysis of metformin in biological fluids could be easily assessed.

3.5. Fouling resistance, stability and selectivity

In order to investigate the fouling resistance of n-NC, consecutive cyclic voltammograms using n-NC in 0.5 mmol L^{-1} metformin solution were recorded. It was observed that the current as well as potential of the peak related to the metformin electrooxidation

Table 2
A comparison between the various methods for quantification of metformin.

Sensing element/method	Linear range (μmol L^{-1})	LOD (μmol L^{-1})	Sensitivity (A (mol L^{-1})$^{-1}$)	Reference
A molecular wire-carbon nanotubes	0.9–50	0.65	0.02	[7]
Capillary electrophoresis	1.9–27.1	0.58	–	[5]
Cu(II) ion/carbon paste electrode	0.2–10	0.07	0.016	[9]
A hanging mercury drop electrode	0.1–2	0.02	0.2	[8]
A potentiometric sensor	51 (lower limit)	5.5	–	[48]
Nickel oxide nanotubes	4.0–63	0.45	0.27	This work

Table 3
Determination and recovery of metformin in commercial tablets.

Sample type	Amount labeled (mg)	Amount added (mg)	Amount found (mg)	Recovery (%)	RSD (%)	Bias (%)
Tablet-1	1000	–	978.34	97.83	3.58	−2.16
Tablet-1	–	1000	979.1	97.91	4.00	−2.09
Tablet-1	–	1000	992.67	99.27	1.69	−0.73
Tablet-2	500	–	501.22	100.24	3.95	0.24
Tablet-2	–	500	502.56	100.51	3.09	0.51
Tablet-2	–	500	485.29	97.06	4.57	−2.94
Tablet-3	500	–	511.98	102.39	1.35	2.39
Tablet-3	–	500	490.99	98.99	3.80	−1.80
Tablet-3	–	500	505.25	101.05	3.99	1.05
Tablet-4	500	–	497.34	99.47	4.45	−0.53
Tablet-4	–	500	503.25	100.65	1.20	0.65
Tablet-4	–	500	490.19	98.04	4.06	−1.96

Table 5
Recovery of metformin in biological fluids.

Sample	Amount added (μmol L^{-1})	Amount found (μmol L^{-1})	Absolute recovery (%)	Mean recovery (%)	RSD (%)
Serum	20	20.23 ± 0.97	102.69	101.15	4.79
	30	30.33 ± 0.40	101.7	101.1	1.32
	40	39.85 ± 1.05	102.44	99.62	2.63
Urine	10	10.33 ± 0.45	108.42	103.3	4.3
	15	15.06 ± 0.35	101.38	100.4	2.3
	20	20.13 ± 0.45	109.44	100.65	2.2
Breast milk	20	21.23 ± 1.79	106.15	107.76	8.43
	30	29.9 ± 0.3	99.66	100.33	1.03
	40	39.13 ± 0.87	97.83	100.59	2.22

changed slightly (<4%) after 50 cyclic scans. This indicates that the intermediate and/or product of the electrooxidation reaction was not adsorbed at the nanocomposite surface and it represented an anti-fouling behavior towards the metformin electrooxidation.

To verify the durability and long-term stability of the nanocomposite, consecutive cyclic voltammograms using n-NC in 100 mmol L^{-1} NaOH solution were recorded. It was found that the peak currents changed slightly (<5%) after 100 cyclic scans. In addition, the electrode was stored in 100 mmol L^{-1} NaOH solution when not in use and retained its electroreactivity for 5 weeks. To verify the fabrication reproducibility of the biosensor, prepared under the same conditions, five n-NC were fabricated and the amperometric responses of the nanocomposite in 0.5 mmol L^{-1} metformin solution were measured. A RSD of 3.8% was obtained indicating that the fabrication method was highly reproducible.

Selectivity of the amperometric method for the assay of the drug was examined in the presence of some common interferences, glucose, L-tyrosine, ascorbic acid, L-serine, sucrose, dopamine and uric acid and some common excipients usually used in pharmaceutical preparations, microcrystalline cellulose, colloidal silicon dioxide, titanium dioxide, talc, starch, and magnesium stearate. The results showed that under the experimental conditions applied in this work, no significant interference was observed for these compounds due to the rejection of the diffusion of these anionic compounds by Nafion membrane.

4. Conclusion

n-NC was prepared with carbon microparticles, Nujol and nickel oxide nanotubes and its electrochemical characteristics were evaluated. Then, the electrooxidation of metformin was studied on n-NC. Metformin was oxidized on n-NC via mediation of Ni(III) active species with a higher rate, in comparison with the "large" counterparts. The kinetic parameters involved in the electrooxidation process (such as the transfer coefficient, the catalytic rate constant, and the diffusion coefficient) were also evaluated. The electrocatalytic oxidation process was diffusion-controlled without any kinetic limitation and fouling effect. An amperometric procedure was optimized and successfully applied for quantification of metformin in bulk form, tablets and human biological fluids. The simplicity, sensitivity, selectivity, and short duration of the analysis are the main advantages of the method.

Acknowledgments

We would like to thank the Research Councils of Islamic Azad University, Shiraz University of Medical Sciences and K. N. Toosi University of Technology and the Iran National Science Foundation (INSF) for supporting this research.

Appendix A. Supplementary data

Supplementary data associated with this article can be found, in the online version, at doi:10.1016/j.talanta.2010.06.022.

References

[1] H.E. Lebovitz, Med. Clin. North Am. 88 (2004) 847.
[2] N. Musi, M.F. Hirshman, J. Nygren, M. Svanfeldt, P. Bavenholm, O. Rooyackers, G. Zhou, J.M. Williamson, O. Ljunqvist, S. Efendic, D.E. Moller, A. Thorell, L. Goodyear, J. Diab. 51 (2002) 2074.
[3] M.S. Lennard, C. Casey, G.T. Tucker, H.F. Woods, Br. J. Clin. Pharmacol. 6 (1978) 183.
[4] S.A. Reuschel, M.E. Arnold, S.E. Liu, S.R.L. Foltz, AAPS Pharm. Sci. 1 (1999) S–308.
[5] J.Z. Song, H.F. Chen, S.J. Tian, Z.P. Sun, J. Chromatogr. B 708 (1998) 277.
[6] J. Martinez Calatayud, P. Campins Falco, M.C. Pascual Marti, Anal. Lett. 18 (1985) 1381.
[7] X.-J. Tian, J.-F. Song, XinJ. Luan, Y.-Y. Wang, Q.-Z. Shi, Anal. Bioanal. Chem. 386 (2006) 2081.
[8] S. Skrzypek, V. Mirceski, W. Ciesielski, A. Sokolowski, R. Zakrzewski, J. Pharm. Biomed. Anal. 45 (2007) 275.
[9] X.-J. Tian, J.-F. Song, J. Pharm. Biomed. Anal. 44 (2007) 1192.
[10] F. Tache, V. David, A. Farca, A. Medvedovici, Microcem. J. 68 (2001) 13.
[11] S. AbuRuz, J. Millership, J. MaElnay, J. Chromatogr. B 798 (2003) 203.
[12] M. Zhang, G.A. Moore, M. Lever, S.J. Gardiner, C.M.J. Kirkpatrick, E.J. Begg, J. Chromatogr. B 766 (2001) 175.
[13] K.H. Yuen, K.K. Peh, J. Chromatogr. B 710 (1998) 243.
[14] O. Vesterquvist, F. Nabbie, B. Swanson, J. Chromatogr. B 716 (1998) 299.
[15] N.C. van de Merbel, G. Wilkens, S. Fowles, B. Oosterhuis, J.H.G. Jonkman, Chromatographia 47 (1998) 542.
[16] F. Tache, V. David, A. Farca, A. Medvedovici, Microcem. J 68 (2001) 13.
[17] J. Keal, A. Somogyi, J. Chromatogr. 378 (1986) 503.
[18] S. AbuRuz, J. Millership, J. MaElnay, J. Chromatogr. B. 798 (2003) 203.
[19] S.A. Ozkan, B. Uslu, H.Y. Aboul-Eneinb, Crit. Rev. Anal. Chem. 33 (2003) 155.
[20] H. Heli, S. Majdi, N. Sattarahmady, A. Parsaei, J. Solid State Electrochem. in press.
[21] H. Yadegari, A. Jabbari, H. Heli, A.A. Moosavi-Movahedi, K. Karimian, A. Khodadadi, Electrochim. Acta 53 (2008) 2907.
[22] S. Majdi, A. Jabbari, H. Heli, H. Yadegari, A.A. Moosavi-Movahedi, S. Haghgoo, J. Solid State Electrochem. 13 (2009) 407.
[23] M.F. Ashby, P.J. Ferreira, D.L. Schodek, Nanomaterials, Nanotechnologies and Design, Elsevier, 2009.
[24] M. Fernandez-Garcia, A. Martinez-Arias, J.C. Hanson, J.A. Rodriguez, Chem. Rev. 104 (2004) 4063.
[25] H. Heli, A. Jabbari, M. Zarghan, A.A. Moosavi-Movahedi, Sens. Actuators B 140 (2009) 245.
[26] H. Heli, M. Hajjizadeh, A. Jabbari, A.A. Moosavi-Movahedi, Biosens. Bioelectron 24 (2009) 2328.
[27] H. Heli, M. Hajjizadeh, A. Jabbari, A.A. Moosavi-Movahedi, Anal. Biochem. 388 (2009) 81.
[28] N. Sattarahmady, H. Heli, A.A. Moosavi-Movahedi, Biosens. Bioelectron 25 (2010) 2329.
[29] S. Zhang, H.C. Zeng, Chem. Mater. 21 (2009) 871.
[30] F.-S. Cai, G.-Y. Zhang, J. Chen, X.L. Gou, H.K. Liu, S.X. Dou, Angew. Chem. 43 (2004) 4212.
[31] P.A. Nelson, J.M. Elliott, G.S. Attard, J.R. Owen, Chem. Mater. 14 (2002) 524.
[32] H. Heli, S. Majdi, N. Sattarahmady, Sens. Actuator B 145 (2010) 185.
[33] H. Heli, F. Faramarzi, N. Sattarahmady, J. Solid State Electrochem. in press.
[34] M. Elkaoutit, I. Naranjo-Rodriguez, M. Dominguez, M.P. Hernandez-Artiga, D. Bellida-Milla, J.L.H.H. de Cisneros, Electrochim. Acta 53 (2008) 7131.
[35] H. Heli, S. Majdi, A. Jabbari, N. Sattarahmady, A.A. Moosavi-Movahedi, J. Solid State Electrochem. 14 (2010) 1515.
[36] H. Heli, A. Jabbari, S. Majdi, M. Mahjoub, A.A. Moosavi-Movahedi, S. Sheibani, J. Solid State Electrochem. 13 (2009) 1951.

[37] M. Hajjizadeh, A. Jabbari, H. Heli, A.A. Moosavi-Movahedi, S. Haghgoo, Electrochim. Acta 53 (2007) 1766.
[38] E. Laviron, J. Electroanal. Chem. 101 (1979) 19.
[39] S. Berchmans, H. Gomathi, G.P. Rao, J. Electroanal. Chem. 394 (1995) 267.
[40] A.J. Bard, L.R. Faulkner, Electrochemical Methods, Wiley, New York, 2001.
[41] N.A. Hampson, J.B. Lee, K.I. Macdonald, J. Electroanal. Chem. 34 (1972) 91.
[42] M. Fleischmann, N. Korinek, D. Pletcher, J. Electroanal. Chem. 31 (1971) 39.
[43] E. Steckham, in: H. Lund, O. Hammerich (Eds.), Organic Electrochemistry, Marcel Dekker, New York, 1991 (chapter 15).
[44] V.B. Kumar, A.E. Bernardo, K. Vyas, M. Franko, S. Farr, L. Lakshmanan, C. Buddhiraju, J.E. Morley, Life Sci. 69 (2001) 2789.
[45] H. Heli, S. Majdi, N. Sattarahmady, Mater. Res. Bull. 45 (2010) 850.
[46] H. Heli, H. Yadegari, Electrochim. Acta 55 (2010) 2139.
[47] J.C. Miller, J.N. Miller, Statistics for Analytical Chemistry, fourth ed., Ellis-Howood, New York, 1994.
[48] S.S.M. Hassana, W.H. Mahmoud, M.A.F. Elmosallamy, A.H.M. Othman, Anal. Chim. Acta 378 (1999) 299.